Journal of
Nanoscience and Nanotechnology
Vol. 11, 11064–11068, 2011

Electrochemical Behavior of Gold Nanoparticles Modified Nitrogen Incorporated Tetrahedral Amorphous Carbon and Its Application in Glucose Sensing

Aiping Liu[1, 2, *], Huaping Wu[3], Xu Qiu[1], and Weihua Tang[1]

[1] *Department of Physics, Center for Optoelectronics Materials and Devices, Zhejiang Sci-Tech University, Xiasha College Park, Hangzhou 310018, China*
[2] *School of Mechanical and Aerospace Engineering, Nanyang Technological University, 50 Nanyang Avenue, Singapore 639798, Singapore*
[3] *Key Laboratory of E&M (Zhejiang University of Technology), Ministry of Education and Zhejiang Province, Hangzhou 310032, Zhejiang, China*

Gold nanoparticles (NPs) with 10–50 nm in diameter were synthesized on nitrogen incorporated tetrahedral amorphous carbon (ta-C:N) thin film electrode by electrodeposition. The deposition and nucleation processes of Au on ta-C:N surface were investigated by cyclic voltammetry and chronoamperometry. The morphology of Au NPs was characterized by scanned electron microscopy. The electrochemical properties of Au NPs modified ta-C:N (ta-C:N/Au) electrode and its ability to sense glucose were investigated by voltammetric and amperometric measurements. The potentiostatic current-time transients showed a progressive nucleation process and diffusion growth of Au on the surface of ta-C:N film according to the Scharifker-Hills model. The Au NPs acted as microelectrodes improved the electron transfer and electrocatalytic oxidation of glucose on ta-C:N electrode. The ta-C:N/Au electrode exhibited fast current response, a linear detection range of glucose from 0.5 to 25 mM and a detection limit of 120 μM, which hinted its potential application as a glucose biosensor.

Keywords: Gold Nanoparticle, Nitrogen Incorporated Tetrahedral Amorphous Carbon, Nucleation Process, Glucose Sensing.

RESEARCH ARTICLE

1. INTRODUCTION

Diabetes is one of the most serious diseases, which is characterized by an abnormal level of blood glucose due to the defects in insulin production and insulin action.[1] Electrochemical glucose sensor has been extensively investigated due to its important applications in clinical diagnosis of diabetes, food analysis and glucose fuel cells.[2, 3] The sensitivity and stability of glucose sensors depend on the physicochemical characteristics of electrode materials employed as a transducer and catalytic activity of redox mediators. Carbon materials, including carbon paste, glassy carbon, pyrolytic graphite, diamond and amorphous carbon, are regarded as ideal electrode materials due to their low cost, wide potential range, low residual current, reproducible surface structure and suitability for chemical modification.[4–6] Among these carbon materials, diamond-based thin films have attracted great attention in the biosensor and biochip applications.[7–9] Furthermore, tetrahedral amorphous carbon (ta-C) or amorphous diamond (a-D) films composed of sp^2 and sp^3 hybridized carbon show high hardness, excellent biocompatibility, chemical inertness and high corrosion resistance similar to diamond films and lower deposition temperature than diamond films.[10] By introducing impurity elements,[11–13] such as nitrogen, phosphorus and nickel, the doped ta-C films possess sufficient conductivity (electrical resistivity 1–10^4 $\Omega \cdot$cm) for electrochemistry, low double layer capacitance, stability in challenging environments, and comparative resistance to fouling deactivation and thus are regarded appropriate for glucose detection. The electron-transfer behavior and electrochemical activity of doped ta-C films can further be enhanced after electrochemical pretreatment or modification using metal nanoparticles (NPs) or nanoclusters.[13–15] Transition metals such as copper, gold, platinum and nickel are known to be active for glucose oxidation in alkaline solutions.[16–18] For

*Author to whom correspondence should be addressed.

 1533-4880/2011/11/11064/005 doi:10.1166/jnn.2011.3935

example, Mena and co-workers designed Au NPs modified glassy carbon electrodes by electrodeposition to detect glucose and analyze kinetic parameters of glucose sensors.[17] Hrapovic et al. prepared Pt NPs with 2–3 μm in diameter on single-wall carbon nanotubes for fabricating electrochemical glucose sensors.[18] However, to our knowledge, there were few reports on glucose oxidation on metallical NPs modified conductive ta-C electrodes.

In the present work, we reported a glucose biosensor based on Au NPs modified nitrogen incorporated ta-C (ta-C:N/Au) thin film. Voltammetric and current transient experiments were carried out to investigate the nucleation and growth processes of Au on ta-C:N surface. The capability of ta-C:N/Au electrode for glucose sensing was confirmed.

2. EXPERIMENTAL DETAILS

2.1. Reagents

D-Glucose (purity 98%) and $HAuCl_4 \cdot 3H_2O$ (purity 99.99%) were supplied by Sigma, USA. All other chemicals were of analytical grade. The water (resistivity > 18 $M\Omega \cdot cm$) was obtained from a Millipore Q purification system.

2.2. Sample Preparation

80-nm ta-C:N films were deposited on *p*-type silicon wafers ($\rho = 0.01$–$0.02\ \Omega \cdot cm$) with 30-sccm N_2 (purity 99.9999%) as the dopant source under a 120 V negative bias using a filtered cathodic vacuum arc system.[13] Au NPs were electrodeposited on as-prepared ta-C:N surfaces in a 0.1 M H_3BO_4 solution containing 0.1 mM $HAuCl_4$ using an electrochemical workstation (CHI 660A, China).[14] The potential was scanned from 0.9 V to −0.1 V (vs. Ag/AgCl (saturated KCl) electrode) and back to 0.9 V for 200 s at 0.02 Vs^{-1}under nitrogen bubbling conditions. The three-electrode system consisted of either a ta-C:N or a ta-C:N/Au working electrode, a Ag/AgCl reference electrode and a Pt foil counter electrode. The exposed area of ta-C:N or ta-C:N/Au in the solution was controlled to be about 0.1 cm^2.

2.3. Electrode Characterization

The composition of ta-C:N film was measured by X-ray photoemission spectroscopy using a PHI ESCA 5700 spectrometer with an Al K_α line (1486.6 eV) as the X-ray source. The content of nitrogen (N/(C + N)) in the ta-C:N film was calculated to be 6.2 at.% from the core level spectra of C 1s and N 1s using the sensitivity factors of the instrument, assuming 1.00 for C and 1.64 for N. The deposition process of Au was analyzed by cyclic voltammetry in a 0.1 M H_2SO_4 solution at different scan rates. The morphology of Au NPs was examined using a Hitachi S4800 scanned electron microscopy (SEM). The nucleation mechanics of Au at the ta-C:N electrode was estimated by chronoamperometry at a potential step from 0.9 V to 0.5 V in a 0.1 M H_3BO_4 solution containing 0.1 mM $HAuCl_4$. Potential pulse width was 100 s and sampling interval was 0.002 s. Glucose detection at the ta-C:N and ta-C:N/Au electrodes was performed in a 0.1 M NaOH solution using the above three-electrode system. A steady-state current-time curve was recorded under an optimal potential with a stirring rate of 300 rpm. Sufficient high-purity N_2 was introduced to the bottom of working solution for about 30 min before experiments. Continuous and slow nitrogen bubbling was controlled to lower the influence of nitrogen flow on signal stability during electrochemical experiments at 25 °C.

3. RESULTS AND DISCUSSION

3.1. Deposition and Nucleation Processes and Morphology of Au NPs

Figure 1 displays the cyclic voltammogram (CV) of ta-C:N/Au electrode in a 0.1 M H_2SO_4 at 0.1 Vs^{-1}. The reduction and oxidation peaks related to Au can be observed at about 0.78 V in the negative scan and 1.40 V on the positive scan, respectively. The reduction of hydrogen ions to hydrogen adatoms occurs at −0.18 V.[19] A linear relation between the reduction peak current of Au and the square root of scan rate, v, (correlation coefficient, $R = 0.9933$) indicates that the reduction process of Au on the ta-C:N electrode is diffusion-controlled (the inset of Fig. 1). The real surface area of Au loading is estimated to be 0.02 cm^2 from the charge consumed in the reduction of the surface oxide monolayer of Au between 0.5 V and 1.1 V in the cathodic scan ($v = 0.1\ Vs^{-1}$) by using the value of 400 $\mu C\ cm^{-2}$.[20,21] Figure 2 illustrates the morphology of Au NPs on the ta-C:N film. The diameter of

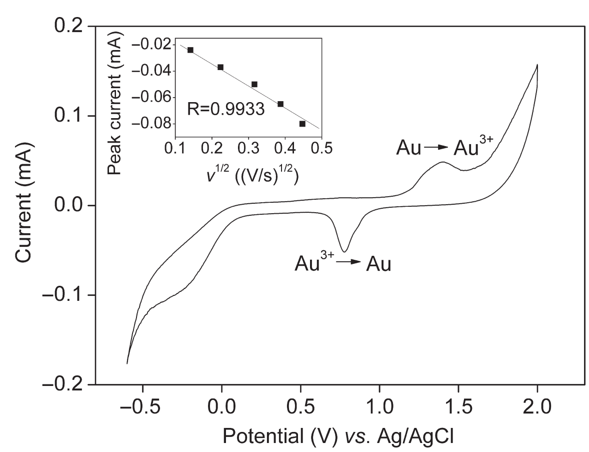

Fig. 1. Cycle voltammogram of ta-C:N/Au electrode in a 0.1 M H_2SO_4 solution at 0.1 Vs^{-1}. The inset shows the linear relation between the cathode peak current of Au and square root of scan rate.

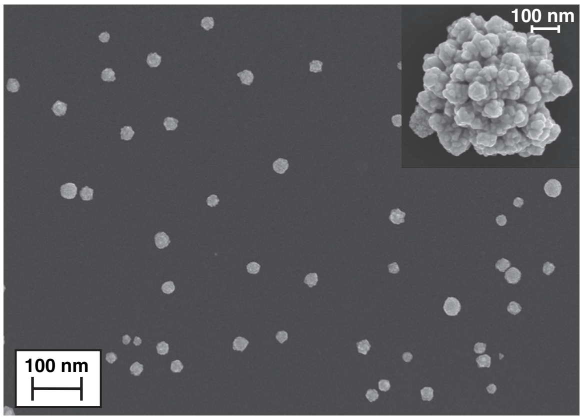

Fig. 2. Scanning electron microscopy image of ta-C:N/Au electrode. The inset shows a cluster of Au NPs.

Au NPs ranges from 10 nm to 50 nm with a density about 2×10^9 per cm^2. Increasing the deposition time can enlarge Au NPs size, forming a flowerlike cluster of Au NPs after 800 s deposition (the inset of Fig. 2).

With the aim to better understand the formation of Au NPs with different sizes, transient current measurement was carried out to analyze the nucleation process of Au. Figure 3(a) shows a typical current (I) versus time (t) profile with a potential step from 0.9 V to 0.5 V in a 0.1 M H_3BO_4 solution containing 0.1 mM $HAuCl_4$. This chronoamperometric curve can be divided into four successive time intervals: the double-layer charging and initial nucleation process at Zone A, the free growth of independent nuclei and formation of new nucleation sites without overlapping at Zone B, the growth of independent nuclei and their overlap at Zone C, and the overlapping of diffusion zones of different nuclei at Zone D. The $I^{1/2}$ versus t plot is linear in Zone B, which indicates a 3D-nucleation process of hemispherical nucleus with diffusion control.[22] According to Scharifker and Hills' viewpoint, there are two kinds of nucleation processes, instantaneous nucleation and progressive nucleation, for the diffusion-limited growth.[23] Our current–time curve is further compared with the two limiting mechanisms using the reduced variables I_m and t_m, as shown in Figure 3(b). t_m is the time corresponding to the maximum current I_m in the chronoamperometric curve. The experimental result agrees better with the progressive nucleation mechanism. Similar results had been obtained for Pt electrodeposition on diamond and pyrolytic graphite.[24, 25] New Au nuclei may therefore be continuously formed at a vacant position of ta-C:N surface or existent Au nuclei, forming Au NPs with different diameters.

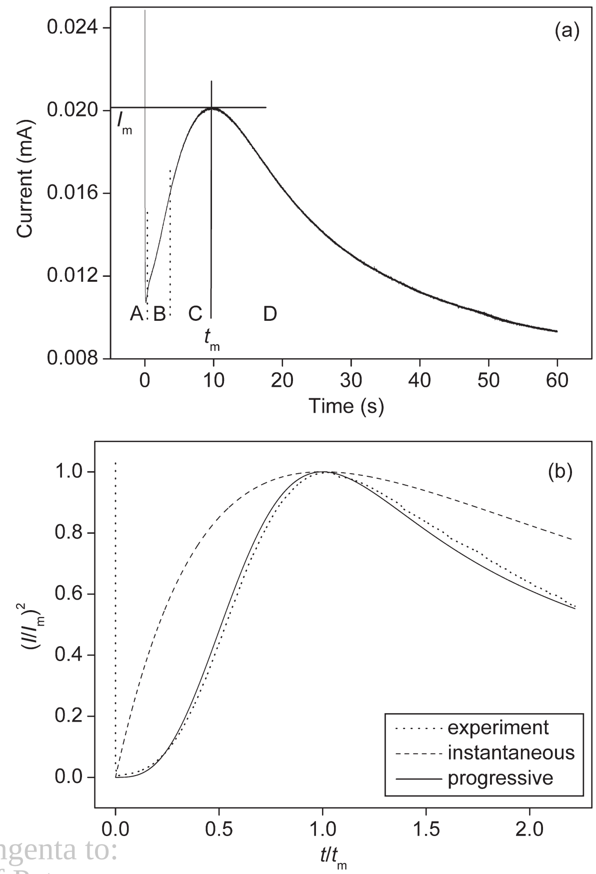

Fig. 3. (a) Chronoamperogram and (b) current-time transient response plotted in reduced variables I/I_m versus t/t_m for Au deposition on the ta-C:N electrode with a potential step from 0.9 V to 0.5 V in a 0.1 M H_3BO_4 solution containing 0.1 mM $HAuCl_4$. The t_m is the time corresponding to the maximum current I_m.

3.2. Glucose Detection on ta-C:N and ta-C:N/Au Electrodes

Figure 4 shows the CVs of glucose oxidation on the ta-C:N/Au electrode. The two peaks at 0.22 V (Peak A) and 0.51 V (Peak B) are attributed to the oxidation peaks of glucose and Au, respectively. During the negative sweep, an intense re-oxidation peak of glucose at about 0.02 V (Peak C) appears in the same potential region as soon as the gold oxides are reduced. However, no obvious response related to glucose oxidation is observed at ta-C:N electrode, hinting a low electrochemical activity of ta-C:N electrode for glucose oxidation (the figure is not shown here). Therefore, the effective electrode surface contributing to glucose oxidation is the area of Au NPs and all currents are normalized to the real surface area of Au, as shown in Figure 4. Increasing the scan rate from 0.05 to 0.2 Vs^{-1} moves Peak A to the positive direction and Peak C to the negative direction. The linear relations between the peak current densities for Peaks A and C and the square root of scan rate, v, suggest diffusion-controlled glucose oxidation at the ta-C:N/Au electrode (the inset of Fig. 4). The reactions occurring at the interface of ta-C:N/Au electrode and working solution can be explained as follows (Parpot proposed).[26] A catalytic hydrous gold oxide, i.e., $AuOH_{ads}$, was formed on the surface of Au NPs after Au/AuO_x NPs had abstracted

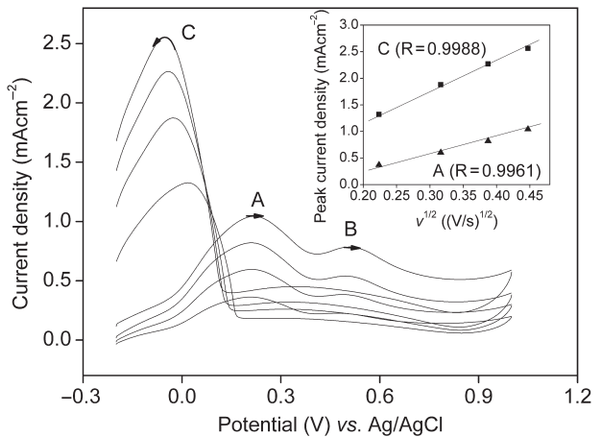

Fig. 4. Cycle voltammograms of glucose oxidation on the ta-C:N/Au electrode in a 0.1 M NaOH solution with 1mM glucose at different scan rates. The inset shows the linear relations between peak current densities of Peaks A and C and square root of scan rate.

hydrogen atoms to yield radicals in the NaOH solution. A glucose molecule then adsorbed onto the AuOH site and transferred an electron to the AuOH site to form gluconate or gluconolactone.[26] Our results indicate that the three-dimensional Au NPs not only accelerate the electron exchange between ta-C:N and glucose but also directly favor glucose oxidation as microelectrodes dispersed on the ta-C:N surface.

Figure 5 shows a typical amperometric response curve of glucose at ta-C:N/Au electrode under 0.22 V with successive increments of 0.5 or 1 mM glucose in the 0.1 M NaOH solution. The electrode response achieves steady-state signal within 8 s. The ta-C:N/Au electrode presents a linear response to glucose oxidation from 0.5 mM to 25 mM with a detection limit of 120 μM based on a

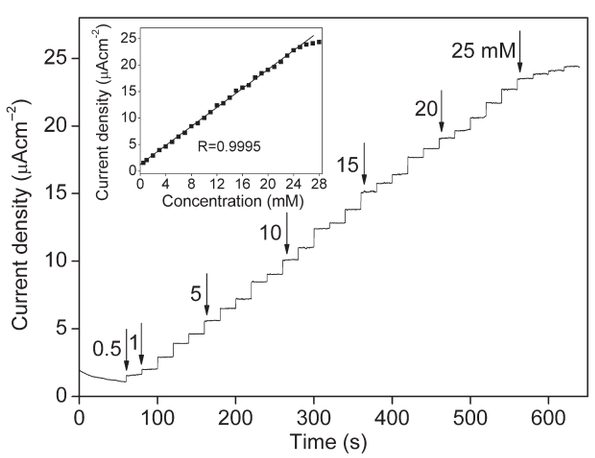

Fig. 5. Current density-time response for glucose oxidation at the ta-C:N/Au electrode with successive addition of 0.5 or 1 mM glucose into the 0.1 M NaOH solution at a potential of 0.22 V. The inset is the relation between the current density and glucose concentration obtained at the ta-C:N/Au electrode.

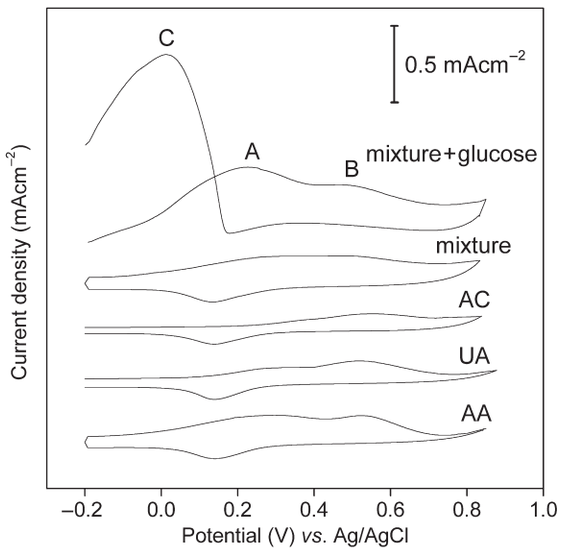

Fig. 6. Cycle voltammograms of 1 mM AA, UA, AC and their mixture without and with 1 mM glucose on the ta-C:N/Au electrode in the 0.1 M NaOH solution.

signal-to-noise ratio of 3. This range is broader than the blood glucose level of a normal human body (3–8 mM). The ta-C:N/Au electrode may further be applied as a glucose-based biosensor due to its immediate response, acceptable sensitivity and wide detection range.

3.3. Selective Detection of Glucose in the Presence of Ascorbic Acid, Uric Acid and Acetaminophen

Ascorbic acid (AA), uric acid (UA) and acetaminophen (AC) existent in blood may interfere with the electrochemical detection of glucose on the ta-C:N/Au electrode when the ta-C:N/Au electrode is used to detect the blood glucose. Figure 6 shows CVs of 1 mM AA, UA, AC and their mixture without and with 1 mM glucose on the ta-C:N/Au electrode in a 0.1 M NaOH solution, respectively. The oxidation peaks of AA, UA and AC are at about 0.30, 0.35 and 0.40 V, respectively. A broad peak at 0.33 V is observed when AA, UA and AC are mixed in the 0.1 M NaOH solution. The oxidation peaks of glucose are still visible when 1 mM glucose is added to the mixture of AA, UA and AC. The ta-C:N/Au electrode has higher catalytic ability for the oxidation of glucose than those of AA, UA and AC at 0.22 V and 0.02 V. Therefore, the ta-C:N/Au electrode may be good for blood glucose determination without obvious interference from AA, UA and AC at least at a lower potential.

4. CONCLUSIONS

Glucose detection using gold nanoparticles (NPs) modified nitrogen incorporated tetrahedral amorphous carbon (ta-C:N/Au) thin film electrode was proposed. The fitting

RESEARCH ARTICLE

of potentiostatic current-time transient with the Scharifker-Hills model showed a progressive nucleation of Au with diffusion-controlled on the ta-C:N surface. The Au NPs significantly improved the electrochemical activity of ta-C:N electrode towards glucose oxidation due to the catalytic action of Au NPs in the alkaline solution. A wide detection range of glucose from 0.5 mM to 25 mM with a low detection limit of 120 μM was obtained using the ta-C:N/Au electrode, which implied that the ta-C:N/Au electrode developed in this study might further be applied as a glucose biosensor due to its instant response, acceptable sensitivity, wide detection range and interference resistance.

Acknowledgments: This work was supported by the National Natural Science Foundation of China (Grant No. 50902123 and Grant No. 11002126), the Project Supported by Zhejiang Provincial Natural Science Foundation of China (Grant No. Y6100425) and the Open Fund of Key Laboratory of Advanced Textile Materials and Manufacturing Technology (Zhejiang Sci-Tech University), Ministry of Education (Grant No. 2009QN02).

References and Notes

1. J. W. Lee and J. D. Helmann, *Diabetes Care* 23, 208 (**2000**).
2. S. Park, H. Boo, and T. D. Chung, *Anal. Chim. Acta* 556, 46 (**2006**).
3. Y. M. Yan, L. Su, and L. Q. Mao, *J. Nanosci. Nanotechnol.* 7, 1625 (**2007**).
4. S. Q. Liu and H. X. Ju, *Biosens. Bioelectron.* 19, 177 (**2003**).
5. R. L. McCreery, *Chem. Rev.* 108, 2646 (**2008**).
6. P. Yang, N. Huang, Y. X. Leng, J. Y. Chen, R. K. Y. Fu, S. C. H. Kwok, Y. Leng, and P. K. Chu, *Biomaterials* 24, 2821 (**2003**).
7. A. Hartl, E. Schmich, J. A. Garrido, J. Hernando, S. C. R. Catharino, S. Walter, P. Feulner, A. Kromka, D. Steinmuller, and M. Stutzmann, *Nat. Mater.* 3, 736 (**2004**).
8. T. N. Rao, I. Yagi, T. Miwa, D. A. Tryk, and A. Fujishima, *Anal. Chem.* 71, 2506 (**1999**).
9. W. Zhao, J. J. Xu, Q. Q. Qiu, and H. Y. Chen, *Biosens. Bioelectron.* 22, 649 (**2006**).
10. J. Robertson, *Mater. Sci. Eng. R* 37, 129 (**2002**).
11. R. G. Compton, J. S. Foord, and F. Marken, *Electroanalysis* 15, 1349 (**2003**).
12. R. Maalouf, H. Chebib, Y. Saikali, O. Vittori, M. Sigaud, F. Garrelie, C. Donnet, and N. Jaffrezic-Renault, *Talanta* 72, 310 (**2007**).
13. A. P. Liu, J. Q. Zhu, J. C. Han, H. P. Wu, and W. Gao, *Electroanalysis* 19, 1773 (**2007**).
14. A. P. Liu, J. Q. Zhu, J. C. Han, H. P. Wu, and C. Z. Jiang, *Electrochem. Commun.* 10, 827 (**2008**).
15. M. Benlahsen, H. Cachet, S. Charvet, C. Debiemme-Chouvy, C. Deslouis, A. Lagrini, and V. Vivier, *Electrochem. Commun.* 7, 496 (**2005**).
16. T. Watanabe, T. A. Ivandini, Y. Makide, A. Fujishima, and Y. Einaga, *Anal. Chem.* 78, 7857 (**2006**).
17. M. L. Mena, P. Yanez-Sedeno, and J. M. Pingarron, *Anal. Biochem.* 336, 20 (**2005**).
18. S. Hrapovic, Y. L. Liu, K. B. Male, and J. H. T. Luong, *Anal. Chem.* 76, 1083 (**2004**).
19. A. C. Hill, R. E. Patterson, J. P. Sefton, and M. R. Columbia, *Langmuir* 15, 4005 (**1999**).
20. A. J. Bard and L. R. Faulkner, Electrochemical Methods: Fundamentals and Application, John Wiley and Sons, New York (**2000**).
21. M. S. El-Deab, T. Okajima, and T. Ohsaka, *J. Electrochem. Soc.* 150, A851 (**2003**).
22. M. Paunovic and M. Schlesinger, Fundamentals of Electrochemical Deposition, John Wiley and Sons, New York (**1998**).
23. B. Scharifker and G. Hills, *Electrochim. Acta* 28, 879 (**1983**).
24. F. Montilla, E. Morallon, I. Duo, Ch. Comninellis, and J. L. Vazquez, *Electrochim. Acta* 48, 3891 (**2003**).
25. G. J. Lu and G. Zangari, *J. Phys, Chem. B* 109, 7998 (**2005**).
26. P. Parpot, S. G. Pires, and A. P. Bettencourt, *J. Electroanal. Chem.* 566, 401 (**2004**).

Received: 30 December 2009. Revised/Accepted: 30 August 2010.

RESEARCH ARTICLE